

Evidence from Type Ia Supernovae for an Accelerating Universe

Alexei V. Filippenko*

*Department of Astronomy, University of California, Berkeley, CA 94720-3411
(alex@astro.berkeley.edu)*

Adam G. Riess*

*Space Telescope Science Institute, 3700 San Martin Dr., Baltimore, MD 21218
(ariess@stsci.edu)*

(**On behalf of the High- z Supernova Search Team*)

Abstract. We review the use of Type Ia supernovae for cosmological distance determinations. Low-redshift SNe Ia ($z \lesssim 0.1$) demonstrate that the Hubble expansion is linear, that $H_0 = 65 \pm 2$ (statistical) $\text{km s}^{-1} \text{Mpc}^{-1}$, and that the properties of dust in other galaxies are similar to those of dust in the Milky Way. We find that the light curves of high-redshift ($z = 0.3\text{--}1$) SNe Ia are stretched in a manner consistent with the expansion of space; similarly, their spectra exhibit slower temporal evolution (by a factor of $1+z$) than those of nearby SNe Ia. The luminosity distances of our first set of 16 high-redshift SNe Ia are, on average, 10–15% farther than expected in a low mass-density ($\Omega_M = 0.2$) universe without a cosmological constant. Preliminary analysis of our second set of 9 SNe Ia is consistent with this. Our work supports models with positive cosmological constant and a current acceleration of the expansion. We address the main potential sources of systematic error; at present, none of them appears to reconcile the data with $\Omega_\Lambda = 0$ and $q_0 \geq 0$. The dynamical age of the Universe is estimated to be 14.2 ± 1.7 Gyr, consistent with the ages of globular star clusters.

INTRODUCTION

Supernovae (SNe) come in two main varieties (see reference [1] for a review). Those whose optical spectra exhibit hydrogen are classified as Type II, while hydrogen-deficient SNe are designated Type I. SNe I are further subdivided according to the appearance of the early-time spectrum: SNe Ia are characterized by strong absorption near 6150 Å (now attributed to Si II), SNe Ib lack this feature but instead show prominent He I lines, and SNe Ic have neither the Si II nor the He I

lines. SNe Ia are believed to result from the thermonuclear disruption of carbon-oxygen white dwarfs, while SNe II come from core collapse in massive supergiant stars. The latter mechanism probably produces most SNe Ib/Ic as well, but the progenitor stars previously lost their outer layers of hydrogen or even helium.

It has long been recognized that SNe Ia may be very useful distance indicators for a number of reasons; see [2,3], and references therein). (1) They are exceedingly luminous, with peak absolute blue magnitudes averaging -19.2 if the Hubble constant, H_0 , is $65 \text{ km s}^{-1} \text{ Mpc}^{-1}$. (2) “Normal” SNe Ia have small dispersion among their peak absolute magnitudes ($\sigma \lesssim 0.3$ mag). (3) Our understanding of the progenitors and explosion mechanism of SNe Ia is on a reasonably firm physical basis. (4) Little cosmic evolution is expected in the peak luminosities of SNe Ia, and it can be modeled. This makes SNe Ia superior to galaxies as distance indicators. (5) One can perform *local* tests of various possible complications and evolutionary effects by comparing nearby SNe Ia in different environments.

Research on SNe Ia in the 1990s has demonstrated their enormous potential as cosmological distance indicators. Although there are subtle effects that must indeed be taken into account, it appears that SNe Ia provide among the most accurate values of H_0 , q_0 (the deceleration parameter), Ω_M (the matter density), and Ω_Λ (the cosmological constant, $\Lambda c^2/3H_0^2$).

There are now two major teams involved in the systematic investigation of high-redshift SNe Ia for cosmological purposes. The “Supernova Cosmology Project” (SCP) is led by Saul Perlmutter of the Lawrence Berkeley Laboratory, while the “High-Z Supernova Search Team” (HZT) is led by Brian Schmidt of the Mt. Stromlo and Siding Springs Observatories. One of us (A.V.F.) has worked with both teams, but his primary allegiance is now with the HZT. In this paper we present results from the HZT.

HOMOGENEITY AND HETEROGENEITY

The traditional way in which SNe Ia have been used for cosmological distance determinations has been to assume that they are perfect “standard candles” and to compare their observed peak brightness with those of SNe Ia in galaxies whose distances have been independently determined (e.g., Cepheids). The rationale is that SNe Ia exhibit relatively little scatter in their peak blue luminosity ($\sigma_B \approx 0.4$ – 0.5 mag; [4]), and even less if “peculiar” or highly reddened objects are eliminated from consideration by using a color cut. Moreover, the optical spectra of SNe Ia are usually rather homogeneous, if care is taken to compare objects at similar times relative to maximum brightness ([5] and references therein). Over 80% of all SNe Ia discovered through the early 1990s were “normal” [6].

From a Hubble diagram constructed with unreddened, moderately distant SNe Ia ($z \lesssim 0.1$) for which peculiar motions should be small and relative distances (as given by ratios of redshifts) are accurate, Vaughan *et al.* [7] find that

$$\langle M_B(\text{max}) \rangle = (-19.74 \pm 0.06) + 5 \log(H_0/50) \text{ mag.} \quad (1)$$

In a series of papers, Sandage *et al.* [8] and Saha *et al.* [9] combine similar relations with *Hubble Space Telescope (HST)* Cepheid distances to the host galaxies of seven SNe Ia to derive $H_0 = 57 \pm 4 \text{ km s}^{-1} \text{ Mpc}^{-1}$.

Over the past decade it has become clear, however, that SNe Ia do *not* constitute a perfectly homogeneous subclass (e.g., [1,10]). In retrospect this should have been obvious: the Hubble diagram for SNe Ia exhibits scatter larger than the photometric errors, the dispersion actually *rises* when reddening corrections are applied (under the assumption that all SNe Ia have uniform, very blue intrinsic colors at maximum; [11,12]), and there are some significant outliers whose anomalous magnitudes cannot possibly be explained by extinction alone.

Spectroscopic and photometric peculiarities have been noted with increasing frequency in well-observed SNe Ia. A striking case is SN 1991T; its pre-maximum spectrum did not exhibit Si II or Ca II absorption lines, yet two months past maximum brightness the spectrum was nearly indistinguishable from that of a classical SN Ia [13,14]. The light curves of SN 1991T were slightly broader than the SN Ia template curves, and the object was probably somewhat more luminous than average at maximum. The reigning champion of well observed, peculiar SNe Ia is SN 1991bg [15–17]. At maximum brightness it was subluminous by 1.6 mag in V and 2.5 mag in B , its colors were intrinsically red, and its spectrum was peculiar (with a deep absorption trough due to Ti II). Moreover, the decline from maximum brightness was very steep, the I -band light curve did not exhibit a secondary maximum like normal SNe Ia, and the velocity of the ejecta was unusually low. The photometric heterogeneity among SNe Ia is well demonstrated by Suntzeff [18] with five objects having excellent $BVRI$ light curves.

COSMOLOGICAL USES: LOW REDSHIFTS

Although SNe Ia can no longer be considered perfect “standard candles,” they are still exceptionally useful for cosmological distance determinations. Excluding those of low luminosity (which are hard to find, especially at large distances), most of the nearby SNe Ia that had been discovered through the early 1990s were *nearly* standard ([6], but see Li *et al.* [19] for recent evidence of a higher intrinsic peculiarity rate). Also, after many tenuous suggestions (e.g., [20–22]), convincing evidence has finally been found for a *correlation* between light-curve shape and luminosity. Phillips [23] achieved this by quantifying the photometric differences among a set of nine well-observed SNe Ia using a parameter, $\Delta m_{15}(B)$, which measures the total drop (in B magnitudes) from maximum to $t = 15$ days after B maximum. In all cases the host galaxies of his SNe Ia have accurate relative distances from surface brightness fluctuations or from the Tully-Fisher relation. In B , the SNe Ia exhibit a total spread of ~ 2 mag in maximum luminosity, and the intrinsically bright SNe Ia clearly decline more slowly than dim ones. The range in absolute magnitude is smaller in V and I , making the correlation with $\Delta m_{15}(B)$ less steep than in B , but it is present nonetheless.

Using SNe Ia discovered during the Calán/Tololo survey ($z \lesssim 0.1$), Hamuy *et al.* [24,25] confirm and refine the Phillips [23] correlation between $\Delta m_{15}(B)$ and $M_{max}(B, V)$: it is not as steep as had been claimed. Apparently the slope is steep only at low luminosities; thus, objects such as SN 1991bg skew the slope of the best-fitting single straight line. Hamuy *et al.* reduce the scatter in the Hubble diagram of normal, unreddened SNe Ia to only 0.17 mag in B and 0.14 mag in V ; see also [26].

In a similar effort, Riess, Press, & Kirshner [27] show that the luminosity of SNe Ia correlates with the detailed shape of the overall light curve. They form a “training set” of light-curve shapes from 9 well-observed SNe Ia having known relative distances, including very peculiar objects (e.g., SN 1991bg). When the light curves of an independent sample of 13 SNe Ia (the Calán/Tololo survey) are analyzed with this set of basis vectors, the dispersion in the V -band Hubble diagram drops from 0.50 to 0.21 mag, and the Hubble constant rises from 53 ± 11 to 67 ± 7 $\text{km s}^{-1} \text{ Mpc}^{-1}$, comparable to the conclusions of Hamuy *et al.* [24,25]. About half of the rise in H_0 results from a change in the position of the “ridge line” defining the linear Hubble relation, and half is from a correction to the luminosity of some of the local calibrators which appear to be unusually luminous (e.g., SN 1972E).

By using light-curve shapes measured through several different filters, Riess, Press, & Kirshner [28] extend their analysis and objectively eliminate the effects of interstellar extinction: a SN Ia that has an unusually red $B - V$ color at maximum brightness is assumed to be *intrinsically* subluminous if its light curves rise and decline quickly, or of normal luminosity but significantly *reddened* if its light curves rise and decline slowly. With a set of 20 SNe Ia consisting of the Calán/Tololo sample and their own objects, they show that the dispersion decreases from 0.52 mag to 0.12 mag after application of this “multi-color light curve shape” (MLCS) method. The results from a recent, expanded set of nearly 50 SNe Ia indicate that the dispersion decreases from 0.44 mag to 0.15 mag (Figure 1). The resulting Hubble constant is 65 ± 2 (statistical) $\text{km s}^{-1} \text{ Mpc}^{-1}$, with an additional systematic and zero-point uncertainty of ± 5 $\text{km s}^{-1} \text{ Mpc}^{-1}$. Riess *et al.* [28] also show that the Hubble flow is remarkably linear; indeed, SNe Ia now constitute the best evidence for linearity. Finally, they argue that the dust affecting SNe Ia is *not* of circumstellar origin, and show quantitatively that the extinction curve in external galaxies typically does not differ from that in the Milky Way (cf. [2], but see [29]).

The advantage of systematically correcting the luminosities of SNe Ia at high redshifts rather than trying to isolate “normal” ones seems clear in view of evidence that the luminosity of SNe Ia may be a function of stellar population. If the most luminous SNe Ia occur in young stellar populations [24,31,32], then we might expect the mean peak luminosity of high-redshift SNe Ia to differ from that of a local sample. Alternatively, the use of Cepheids (Population I objects) to calibrate local SNe Ia can lead to a zero point that is too luminous. On the other hand, as long as the physics of SNe Ia is essentially the same in young stellar populations locally and at high redshift, we should be able to adopt the luminosity correction methods (photometric and spectroscopic) found from detailed studies of low-redshift SNe Ia.

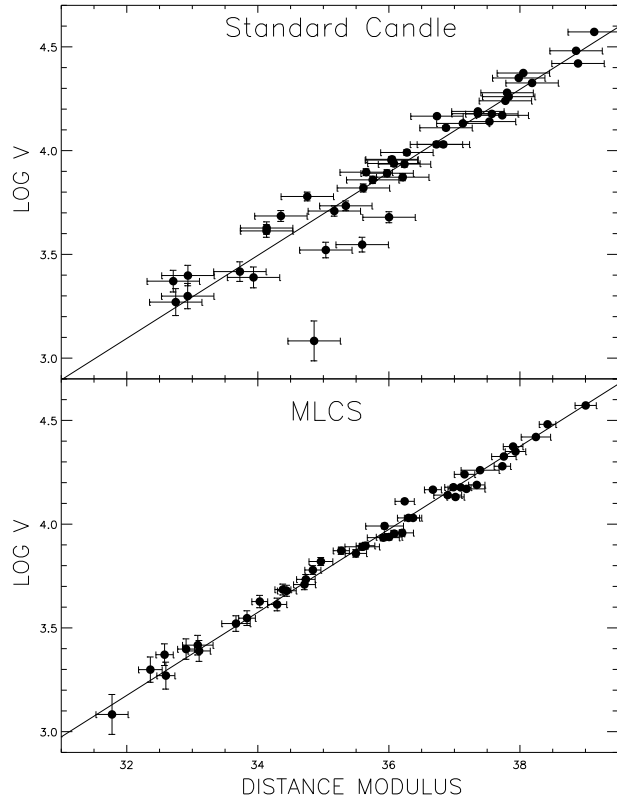


Figure 1: Hubble diagrams for SNe Ia [30] with velocities (km s^{-1}) in the COBE rest frame on the Cepheid distance scale. *Top:* The objects are assumed to be *standard candles* and there is no correction for extinction; the result is $\sigma = 0.42$ mag and $H_0 = 58 \pm 8 \text{ km s}^{-1} \text{ Mpc}^{-1}$. *Bottom:* The same objects, after correction for reddening and intrinsic differences in luminosity. The result is $\sigma = 0.15$ mag and $H_0 = 65 \pm 2$ (statistical) $\text{km s}^{-1} \text{ Mpc}^{-1}$.

Large numbers of nearby SNe Ia are now being found by the Lick Observatory Supernova Search (LOSS) conducted with the 0.76-m Katzman Automatic Imaging Telescope (KAIT; [19,34]). CCD images are taken of about 1000 galaxies per night and compared with KAIT “template images” obtained earlier; the templates are automatically subtracted from the new images and analyzed with computer software. The system reobserves the best candidates the same night, to eliminate star-like cosmic rays, asteroids, and other sources of false alarms. The next day, undergraduate students at UC Berkeley examine all candidates, including weak ones, and they glance at all subtracted images to locate SNe that might be near bright, poorly subtracted stars or galactic nuclei. LOSS discovered 20 SNe (of all types) in 1998 and 40 SNe in 1999, making it the world’s most successful search for nearby SNe. The most important objects were photometrically monitored through *BVRI* (and sometimes *U*) filters (e.g., [33]), and unfiltered follow-up observations were made of all of them during the course of the SN search. This growing sample of

well-observed SNe Ia should allow us to more precisely calibrate the MLCS method, as well as to look for correlations between the observed properties of the SNe and their environment (Hubble type of host galaxy, metallicity, stellar population, etc.).

COSMOLOGICAL USES: HIGH REDSHIFTS

These same techniques can be applied to construct a Hubble diagram with high-redshift SNe Ia, from which the value of q_0 can be determined. With enough objects spanning a range of redshifts, we can determine Ω_M and Ω_Λ independently (e.g., [35]). Contours of peak apparent R -band magnitude for SNe Ia at two redshifts have different slopes in the Ω_M – Ω_Λ plane, and the regions of intersection provide the answers we seek.

The Search

Based on the pioneering work of Norgaard-Nielsen *et al.* [36], whose goal was to find SNe in moderate-redshift clusters of galaxies, the SCP [37] and our HZT [38] devised a strategy that almost guarantees the discovery of many faint, distant SNe Ia on demand, during a predetermined set of nights. This “batch” approach to studying distant SNe allows follow-up spectroscopy and photometry to be *scheduled* in advance, resulting in a systematic study not possible with random discoveries. Most of the searched fields are equatorial, permitting follow-up from both hemispheres.

Our approach is simple in principle; see [38] for details, and for a description of our first high-redshift SN Ia (SN 1995K). Pairs of first-epoch images are obtained with the CTIO or CFHT 4-m telescopes and wide-angle imaging cameras during the nights just after new moon, followed by second-epoch images 3–4 weeks later. (Pairs of images permit removal of cosmic rays, asteroids, and distant Kuiper-belt objects.) These are compared immediately using well-tested software, and new SN candidates are identified in the second-epoch images (Figure 2). Spectra are obtained as soon as possible after discovery to verify that the objects are SNe Ia and determine their redshifts. Each team has already found over 80 SNe in concentrated batches, as reported in numerous *IAU Circulars* (e.g., [39], 11 SNe with $0.16 \lesssim z \lesssim 0.65$; [40], 17 SNe with $0.09 \lesssim z \lesssim 0.84$).

Intensive photometry of the SNe Ia commences within a few days after procurement of the second-epoch images; it is continued throughout the ensuing and subsequent dark runs. In a few cases *HST* images are obtained. As expected, most of the discoveries are *on the rise or near maximum brightness*. When possible, the SNe are observed in filters which closely match the redshifted B and V bands; this way, the K -corrections become only a second-order effect [41]. Custom-designed filters for redshifts centered on 0.35 and 0.45 are used by our HZT [38], when appropriate. We try to obtain excellent *multi-color* light curves, so that reddening and luminosity corrections can be applied [28,31,25].

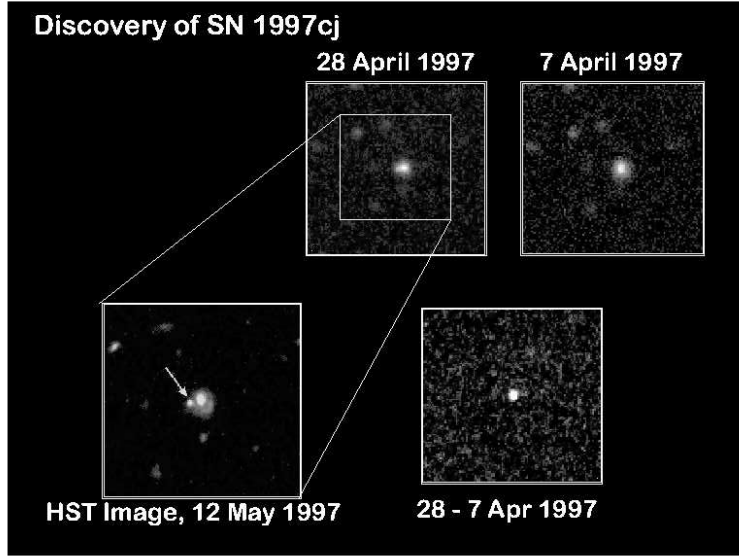


Figure 2: Discovery image of SN 1997cj (28 April 1997), along with the template image (7 April 1997) and an *HST* image obtained subsequently. The net (subtracted) image is also shown.

Although SNe in the magnitude range 22–22.5 can sometimes be spectroscopically confirmed with 4-m class telescopes, the signal-to-noise ratios are low, even after several hours of integration. Certainly Keck is required for the fainter objects (mag 22.5–24.5). With Keck, not only can we rapidly confirm a large number of candidate SNe, but we can search for peculiarities in the spectra that might indicate evolution of SNe Ia with redshift. Moreover, high-quality spectra allow us to measure the age of a supernova: we have developed a method for automatically comparing the spectrum of a SN Ia with a library of spectra corresponding to many different epochs in the development of SNe Ia [5]. Our technique also has great practical utility at the telescope: we can determine the age of a SN “on the fly,” within half an hour after obtaining its spectrum. This allows us to rapidly decide which SNe are best for subsequent photometric follow-up, and we immediately alert our collaborators on other telescopes.

Results

First, we note that the light curves of high-redshift SNe Ia are broader than those of nearby SNe Ia; the initial indications [42,43] are amply confirmed with our larger samples. Quantitatively, the amount by which the light curves are “stretched” is consistent with a factor of $1 + z$, as expected if redshifts are produced by the expansion of space rather than by “tired light.” We were also able to demonstrate this *spectroscopically* at the 2σ confidence level for a single object: the spectrum

of SN 1996bj ($z = 0.57$) evolved more slowly than those of nearby SNe Ia, by a factor consistent with $1 + z$ [5]. More recently, we have used observations of SN 1997ex ($z = 0.36$) at three epochs to conclusively verify the effects of time dilation: temporal changes in the spectra are slower than those of nearby SNe Ia by roughly the expected factor of 1.36 [44].

Following our Spring 1997 campaign, in which we found a SN with $z = 0.97$ (SN 1997ck), and for which we obtained *HST* follow-up images of three SNe, we published our first substantial results concerning the density of the Universe [45]: $\Omega_M = 0.35 \pm 0.3$ under the *assumption* that $\Omega_{\text{total}} = 1$, or $\Omega_M = -0.1 \pm 0.5$ under the *assumption* that $\Omega_\Lambda = 0$. Our independent analysis of 10 SNe Ia using the “snapshot” distance method (with which conclusions are drawn from sparsely observed SNe Ia) gives quantitatively similar conclusions [46].

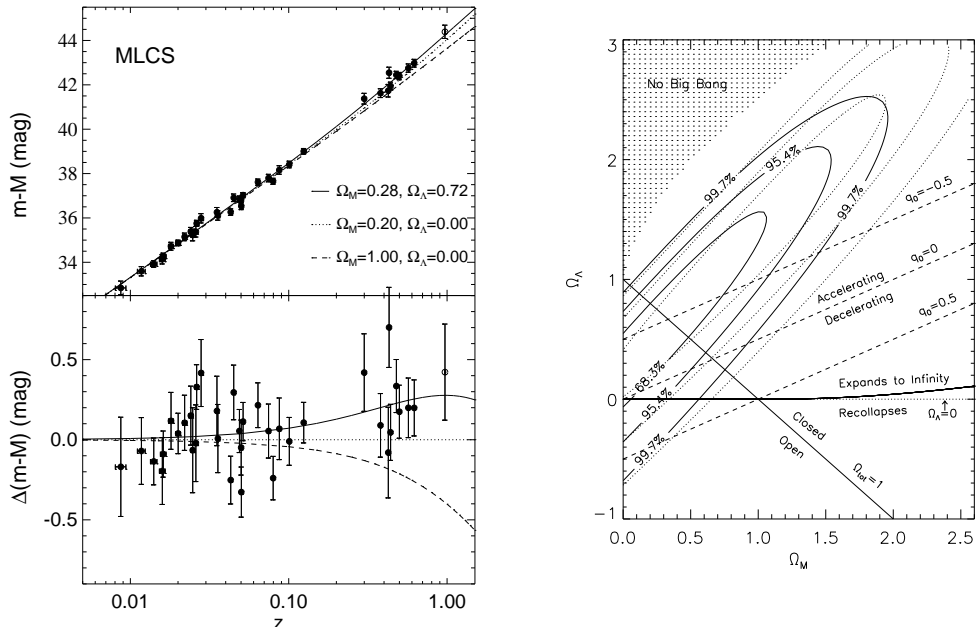


Figure 3 (left): The upper panel shows the Hubble diagram for the low-redshift and high-redshift SN Ia samples with distances measured from the MLCS method; see [48]. Overplotted are three world models: “low” and “high” Ω_M with $\Omega_\Lambda = 0$, and the best fit for a flat universe ($\Omega_M = 0.28$, $\Omega_\Lambda = 0.72$). The bottom panel shows the difference between data and models from the $\Omega_M = 0.20$, $\Omega_\Lambda = 0$ prediction. Except for SN 1997ck (*open symbol*; $z = 0.97$), which lacks spectroscopic confirmation and was excluded from the fit, only the 9 best-observed high-redshift SNe Ia are shown. The average difference between the data and the $\Omega_M = 0.20$, $\Omega_\Lambda = 0$ prediction is 0.25 mag.

Figure 4 (right): Joint confidence intervals for $(\Omega_M, \Omega_\Lambda)$ from SNe Ia [48]. The solid contours are results from the MLCS method applied to 10 well-observed SN Ia light curves, together with the snapshot method [46] applied to 6 incomplete SN Ia light curves. The dotted contours are for the same objects excluding SN 1997ck ($z = 0.97$). Regions representing specific cosmological scenarios are illustrated.

Our next results, obtained from a total of 16 high- z SNe Ia, were announced at a conference in February 1998 [47] and formally published by Riess *et al.* [48] in September 1998. The Hubble diagram (from a refined version of the MLCS method [48]) for the 10 best-observed high- z SNe Ia is given in Figure 3, while Figure 4 illustrates the derived confidence contours in the Ω_M – Ω_Λ plane. We confirm our previous suggestion that Ω_M is low. Even more exciting, however, is our conclusion that Ω_Λ is *nonzero* at the 3σ statistical confidence level. With the MLCS method applied to the full set of 16 SNe Ia, our formal results are $\Omega_M = 0.24 \pm 0.10$ if $\Omega_{\text{total}} = 1$, or $\Omega_M = -0.35 \pm 0.18$ (unphysical) if $\Omega_\Lambda = 0$. If we demand that $\Omega_M = 0.2$, then the best value for Ω_Λ is 0.66 ± 0.21 . These conclusions do not change significantly if only the 9 best-observed SNe Ia are used (Figure 3; $\Omega_M = 0.28 \pm 0.10$ if $\Omega_{\text{total}} = 1$). The $\Delta m_{15}(B)$ method yields similar results; if anything, the case for a positive cosmological constant strengthens. (For brevity, in this paper we won't quote the $\Delta m_{15}(B)$ numbers; see [48] for details.) From an essentially independent set of 42 high- z SNe Ia (only 2 objects in common), the SCP obtains almost identical results [49]. This suggests that neither team has made a large, simple blunder!

Recently, we have calibrated an additional sample of 9 high- z SNe Ia, including several observed with *HST*. Preliminary analysis suggests that the new data are entirely consistent with the old results, thereby strengthening their statistical significance. Figure 5 shows the tentative Hubble diagram; full details will be published elsewhere.

Though not drawn in Figure 4, the expected confidence contours from measurements of the angular scale of the first acoustic peak of the cosmic microwave background radiation (CMBR) are nearly perpendicular to those provided by SNe Ia (e.g., [50,51]); thus, the two techniques provide complementary information. A stunning result was already available by mid-1998 from existing measurements [52,55]: our analysis of the data in [48] demonstrates that $\Omega_M + \Omega_\Lambda = 0.94 \pm 0.26$, when the SN and CMBR constraints are combined [54] (see also [55,56], and others). As shown in Figure 6, the confidence contours are nearly circular, instead of highly eccentric ellipses as in Figure 4. Just a few days before the Second Tropical Workshop, the more accurate and precise results of the BOOMERANG collaboration were announced [57], and shortly thereafter the MAXIMA collaboration distributed their very similar findings [58,59]; the TOCO measurements [60] are also relevant. The bottom line is that we appear to live in a flat universe: $\Omega_{\text{total}} = 1$. Combined with the supernova results, the evidence for nonzero Ω_Λ is strong. Making the argument even more compelling is the fact that various studies of clusters of galaxies (see summary by [61]) show that $\Omega_M \approx 0.3$, so if the CMBR results are correct, one is led to the independent conclusion that $\Omega_\Lambda > 0$. We eagerly look forward to future CMBR measurements of even greater precision.

The dynamical age of the Universe can be calculated from the cosmological parameters. In an empty Universe with no cosmological constant, the dynamical age is simply the “Hubble time” (i.e., the inverse of the Hubble constant); there is no deceleration. SNe Ia yield $H_0 = 65 \pm 2 \text{ km s}^{-1} \text{ Mpc}^{-1}$ (statistical uncertainty only), and a Hubble time of 15.1 ± 0.5 Gyr. For a more complex cosmology, integrating

the velocity of the expansion from the current epoch ($z = 0$) to the beginning ($z = \infty$) yields an expression for the dynamical age. As shown in detail by Riess *et al.* [48], we obtain a value of $14.2^{+1.0}_{-0.8}$ Gyr using the likely range for $(\Omega_M, \Omega_\Lambda)$ that we measure. (The precision is so high because our experiment is sensitive to roughly the *difference* between Ω_M and Ω_Λ , and the dynamical age also varies in approximately this way.) Including the *systematic* uncertainty of the Cepheid distance scale, which may be up to 10%, a reasonable estimate of the dynamical age is 14.2 ± 1.7 Gyr.

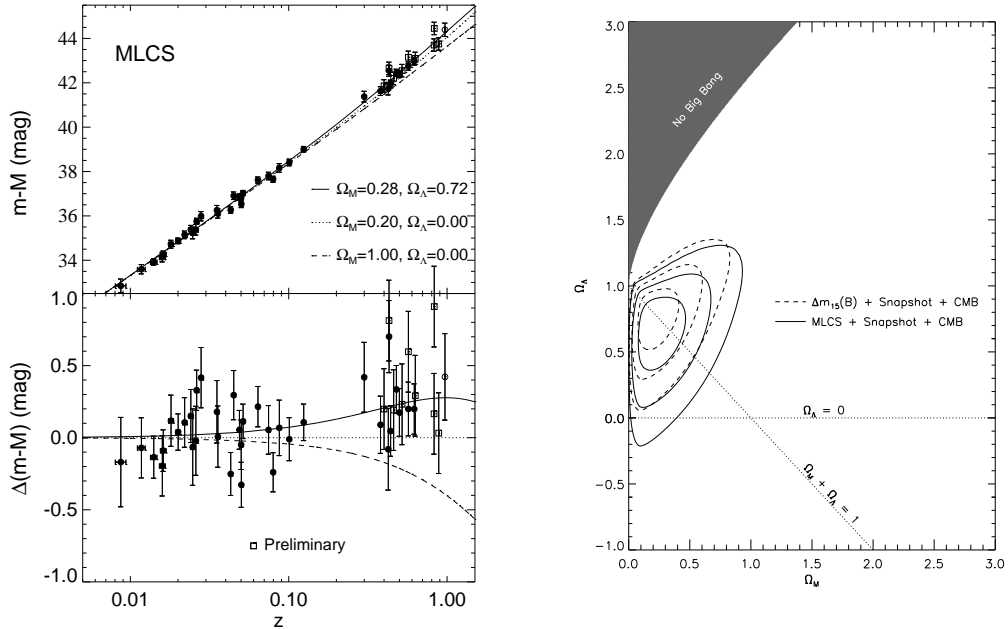


Figure 5 (left): As in Figure 3, the upper panel shows the Hubble diagram for the low- z and high- z SN Ia samples. Here, we include preliminary analysis of 9 additional SNe Ia (*open squares*). The bottom panel shows the difference between data and models from the $\Omega_M = 0.20, \Omega_\Lambda = 0$ prediction.

Figure 6 (right): The HZT's combined constraints from SNe Ia (Figure 3) and the position of the first acoustic peak of the CMB angular power spectrum, based on data available in mid-1998; see [54]. The contours mark the 68%, 95.4%, and 99.7% enclosed probability regions. Solid curves correspond to results from the MLCS method, while dotted ones are from the $\Delta m_{15}(B)$ method; all 16 SNe Ia in [48] were used.

This result is consistent with ages determined from various other techniques such as the cooling of white dwarfs (Galactic disk > 9.5 Gyr [62]), radioactive dating of stars via the thorium and europium abundances (15.2 ± 3.7 Gyr [63]), and studies of globular clusters (10–15 Gyr, depending on whether *Hipparcos* parallaxes of Cepheids are adopted [64,65]). Evidently, there is no longer a problem that the age of the oldest stars seems greater than the dynamical age of the Universe.

DISCUSSION

High-redshift SNe Ia are observed to be dimmer than expected in an empty Universe (i.e., $\Omega_M = 0$) with no cosmological constant. A cosmological explanation for this observation is that a positive vacuum energy density accelerates the expansion. Mass density in the Universe exacerbates this problem, requiring even more vacuum energy. For a Universe with $\Omega_M = 0.2$, the average MLCS distance moduli of the well-observed SNe are 0.25 mag larger (i.e., 12.5% greater distances) than the prediction from $\Omega_\Lambda = 0$. The average MLCS distance moduli are still 0.18 mag bigger than required for a 68.3% (1σ) consistency in a universe with $\Omega_M = 0.2$ and without a cosmological constant. The derived value of q_0 is -0.75 ± 0.32 , implying that the expansion of the Universe is accelerating. If Ω_Λ really is constant, then at least the region of the Universe we have observed ($z \lesssim 0.8$) will expand eternally. Under the simplifying assumption of global homogeneity and isotropy, the entire Universe will behave in this manner.

A very important point is that the dispersion in the peak luminosities of SNe Ia ($\sigma = 0.15$ mag) is low after application of the MLCS method of [28,48]. With 16 SNe Ia, our effective uncertainty is $0.15/4 \approx 0.04$ mag, less than the expected difference of 0.25 mag between universes with $\Omega_\Lambda = 0$ and 0.76 (and low Ω_M); see Figure 3. Systematic uncertainties of even 0.05 mag (e.g., in the extinction) are significant, and at 0.1 mag they dominate any decrease in statistical uncertainty gained with a larger sample of SNe Ia. Thus, our conclusions with only 16 SNe Ia are already limited by systematic uncertainties, *not* by statistical uncertainties — but of course the 9 new objects further strengthen our case.

Here we explore the major possible systematic effects that could invalidate our results. Of those that can be quantified at the present time, none appears to reconcile the data with $\Omega_\Lambda = 0$, though further work is necessary to verify this. Additional details can be found in [38] and especially [48].

Evolution

Perhaps the most obvious possible culprit is *evolution* of SNe Ia over cosmic time, due to changes in metallicity, progenitor mass, or some other factor. If the peak luminosity of SNe Ia were lower at high redshift, then the case for $\Omega_\Lambda > 0$ would weaken. Conversely, if the distant explosions are more powerful, then the case for acceleration strengthens. Theorists are not yet sure what the sign of the effect will be, if it's present at all; different assumptions lead to different conclusions [66–70].

Of course, it is very difficult to obtain an independent measure of the peak luminosity of high- z SNe Ia, and hence to directly test for luminosity evolution. However, we can more easily determine whether *other* observable properties of low- z and high- z SNe Ia differ. If they are all the same, it is more probable that the peak luminosity is constant as well — but if they differ, then the peak luminosity might also be affected (e.g., [66]). Drell *et al.* [71], for example, argue that there are

reasons to suspect evolution, because the average properties of existing samples of high- z and low- z SNe Ia seem to differ (e.g., the high- z SNe Ia are more uniform).

The local sample of SNe Ia displays a weak correlation between light-curve shape (or luminosity) and host galaxy type, in the sense that the most luminous SNe Ia with the broadest light curves only occur in late-type galaxies. Both early-type and late-type galaxies provide hosts for dimmer SNe Ia with narrower light curves [31]. The mean luminosity difference for SNe Ia in late-type and early-type galaxies is ~ 0.3 mag. In addition, the SN Ia rate per unit luminosity is almost twice as high in late-type galaxies as in early-type galaxies at the present epoch [72]. These results may indicate an evolution of SNe Ia with progenitor age. Possibly relevant physical parameters are the mass, metallicity, and C/O ratio of the progenitor [66].

We expect that the relation between light-curve shape and luminosity that applies to the range of stellar populations and progenitor ages encountered in the late-type and early-type hosts in our nearby sample should also be applicable to the range we encounter in our distant sample. In fact, the range of age for SN Ia progenitors in the nearby sample is likely to be *larger* than the change in mean progenitor age over the 4–6 Gyr lookback time to the high- z sample. Thus, to first order at least, our local sample should correct our distances for progenitor or age effects.

We can place empirical constraints on the effect that a change in the progenitor age would have on our SN Ia distances by comparing subsamples of low-redshift SNe Ia believed to arise from old and young progenitors. In the nearby sample, the mean difference between the distances for the early-type (8 SNe Ia) and late-type hosts (19 SNe Ia), at a given redshift, is 0.04 ± 0.07 mag from the MLCS method. This difference is consistent with zero. Even if the SN Ia progenitors evolved from one population at low redshift to the other at high redshift, we still would not explain the surplus in mean distance of 0.25 mag over the $\Omega_\Lambda = 0$ prediction.

Moreover, it is reassuring that initial comparisons of high-redshift SN Ia spectra appear remarkably similar to those observed at low redshift. For example, the spectral characteristics of SN 1998ai ($z = 0.49$) appear to be essentially indistinguishable from those of normal low-redshift SNe Ia; see Figure 7. In fact, the most obviously discrepant spectrum in this figure is the second one from the top, that of SN 1994B ($z = 0.09$); it is intentionally included as a “decoy” that illustrates the degree to which even the spectra of nearby, relatively normal SNe Ia can vary. Nevertheless, it is important to note that a dispersion in luminosity (perhaps 0.2 mag) exists even among the other, more normal SNe Ia shown in Figure 7; thus, our spectra of SN 1998ai and other high-redshift SNe Ia are not yet sufficiently good for independent, *precise* determinations of luminosity from spectral features [73]. Many of them, however, are sufficient for ruling out other supernovae types (Figure 8), or for identifying gross peculiarities such as those shown by SNe 1991T and 1991bg; see Coil *et al.* [74].

We can help verify that the SNe at $z \approx 0.5$ being used for cosmology do not belong to a subluminous population of SNe Ia by examining restframe I -band light curves. Normal, nearby SNe Ia show a pronounced second maximum in the I band about a month after the first maximum and typically about 0.5 mag fainter (e.g.,

[75,18]). Subluminous SNe Ia, in contrast, do not show this second maximum, but rather follow a linear decline or show a muted second maximum [15]. As discussed by Riess *et al.* [76], some evidence for the second maximum is seen from our existing *J*-band (restframe *I*-band) data on SN 1999Q ($z = 0.46$); see Figure 9. However, better data on more SNe Ia are needed to confirm the effect.

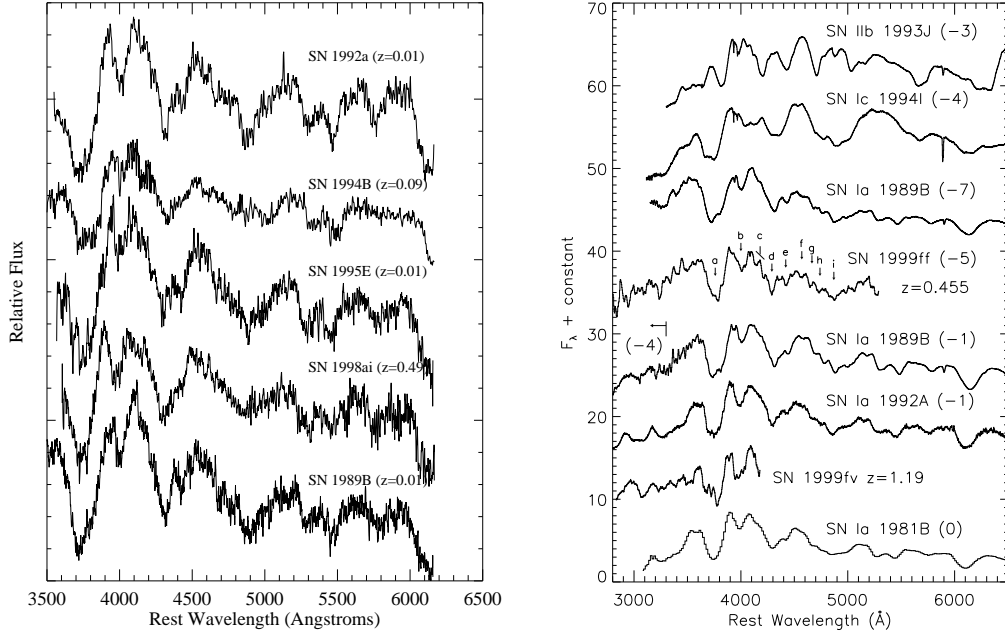


Figure 7 (left): Spectral comparison (in f_λ) of SN 1998ai ($z = 0.49$; Keck spectrum) with low-redshift ($z < 0.1$) SNe Ia at a similar age (~ 5 days before maximum brightness), from [48]. The spectra of the low-redshift SNe Ia were resampled and convolved with Gaussian noise to match the quality of the spectrum of SN 1998ai. Overall, the agreement in the spectra is excellent, tentatively suggesting that distant SNe Ia are physically similar to nearby SNe Ia. SN 1994B ($z = 0.09$) differs the most from the others, and was included as a “decoy.”

Figure 8 (right): Heavily smoothed spectra of two high- z SNe (SN 1999ff at $z = 0.455$ and SN 1999fv at $z = 1.19$; quite noisy below ~ 3500 Å) are presented along with several low- z SN Ia spectra (SNe 1989B, 1992A, and 1981B), a SN Ib spectrum (SN 1993J), and a SN Ic spectrum (SN 1994I); see [1] for a discussion of spectra of various types of SNe. The date of the spectra relative to *B*-band maximum is shown in parentheses after each object’s name. Specific features seen in SN 1999ff and labeled with a letter are discussed by Coil *et al.* [74]. This comparison shows that the two high- z SNe are most likely SNe Ia.

Another way of using light curves to test for possible evolution of SNe Ia is to see whether the rise time (from explosion to maximum brightness) is the same for high- z and low- z SNe Ia; a difference might indicate that the peak luminosities are

also different [66]. We recently measured the risetime of nearby SNe Ia, using data from KAIT, the Beijing Astronomical Observatory (BAO) SN search, and a few amateur astronomers [77]. Though the exact value of the risetime is a function of peak luminosity, for typical low- z SNe Ia we find 20.0 ± 0.2 days. We pointed out [78] that this differs by 5.8σ from the *preliminary* risetime of 17.5 ± 0.4 days reported in conferences by the SCP [79–81]. However, a more thorough analysis of the SCP data [82] shows that the high- z uncertainty of ± 0.4 days that the SCP originally reported was much too small because it did not account for systematic effects. The revised discrepancy with the low- z risetime is about 2σ or less. Thus, the apparent difference in risetimes might be insignificant. Even if the difference is real, however, its relevance to the peak luminosity is unclear; the light curves may differ only in the first few days after the explosion, and this could be caused by small variations in conditions near the outer part of the exploding white dwarf that are inconsequential at the peak.

Extinction

Our SN Ia distances have the important advantage of including corrections for interstellar extinction occurring in the host galaxy and the Milky Way. Extinction corrections based on the relation between SN Ia colors and luminosity improve distance precision for a sample of nearby SNe Ia that includes objects with substantial extinction [28]; the scatter in the Hubble diagram is much reduced. Moreover, the consistency of the measured Hubble flow from SNe Ia with late-type and early-type hosts (see above) shows that the extinction corrections applied to dusty SNe Ia at low redshift do not alter the expansion rate from its value measured from SNe Ia in low dust environments.

In practice, our high-redshift SNe Ia appear to suffer negligible extinction; their $B - V$ colors at maximum brightness are normal, suggesting little color excess due to reddening. Riess, Press, & Kirshner [83] found indications that the Galactic ratios between selective absorption and color excess are similar for host galaxies in the nearby ($z \leq 0.1$) Hubble flow. Yet, what if these ratios changed with lookback time (e.g., [84])? Could an evolution in dust grain size descending from ancestral interstellar “pebbles” at higher redshifts cause us to underestimate the extinction? Large dust grains would not imprint the reddening signature of typical interstellar extinction upon which our corrections rely.

However, viewing our SNe through such gray interstellar grains would also induce a *dispersion* in the derived distances. Using the results of Hatano, Branch, & Deaton [85], Riess *et al.* [48] estimate that the expected dispersion would be 0.40 mag if the mean gray extinction were 0.25 mag (the value required to explain the measured MLCS distances without a cosmological constant). This is significantly larger than the 0.21 mag dispersion observed in the high-redshift MLCS distances. Furthermore, most of the observed scatter is already consistent with the estimated *statistical* errors, leaving little to be caused by gray extinction. Nevertheless, if we

assumed that *all* of the observed scatter were due to gray extinction, the mean shift in the SN Ia distances would only be 0.05 mag. With the observations presented here, we cannot rule out this modest amount of gray interstellar extinction.

Gray *intergalactic* extinction could dim the SNe without either telltale reddening or dispersion, if all lines of sight to a given redshift had a similar column density of absorbing material. The component of the intergalactic medium with such uniform coverage corresponds to the gas clouds producing Lyman- α forest absorption at low redshifts. These clouds have individual H I column densities less than about 10^{15} cm^{-2} [86]. However, they display low metallicities, typically less than 10% of solar. Gray extinction would require larger dust grains which would need a larger mass in heavy elements than typical interstellar grain size distributions to achieve a given extinction. It is possible that large dust grains are blown out of galaxies by radiation pressure, and are therefore not associated with Lyman- α clouds [87].

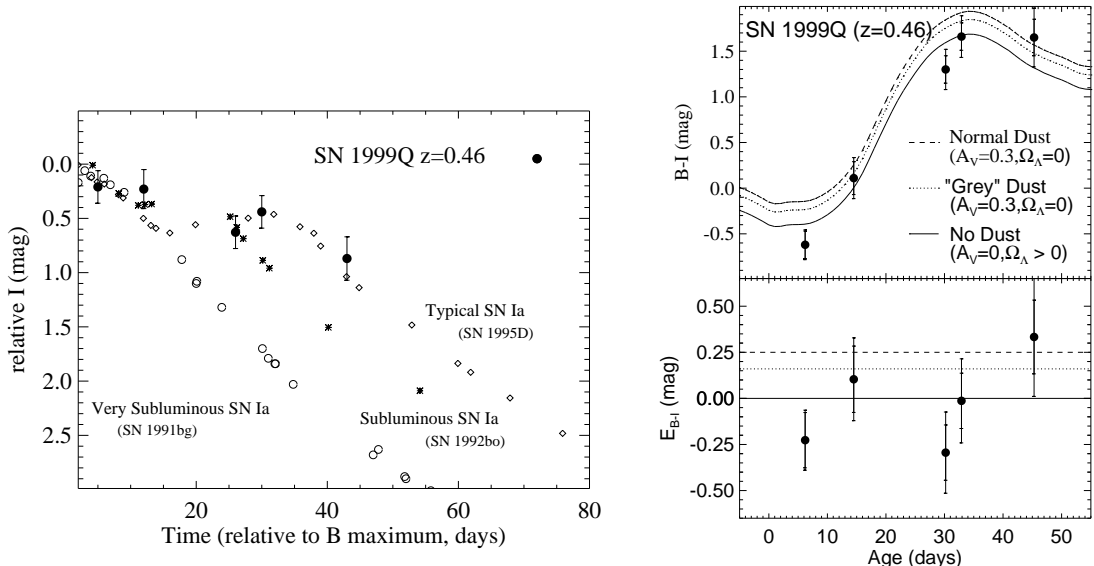


Figure 9 (left): Restframe I -band (observed J -band) light curve of SN 1999Q ($z = 0.46$, 5 solid points; [76]), superposed on the I -band light curves of several nearby SNe Ia. Subluminous SNe Ia exhibit a less prominent second maximum than do normal SNe Ia.

Figure 10 (right): Color excess, E_{B-I} , for SN 1999Q and different dust models [76]. The data are most consistent with no dust and $\Omega_\Lambda > 0$.

But even the dust postulated by Aguirre [84,87,88] is not *completely* gray, having a size of about $0.1 \mu\text{m}$. We can test for such nearly gray dust by observing high-redshift SNe Ia over a wide wavelength range to measure the color excess it would introduce. If $A_V = 0.25$ mag, then $E(U - I)$ and $E(B - I)$ should be 0.12–0.16 mag [84,87]. If, on the other hand, the 0.25 mag faintness is due to Λ , then no such reddening should be seen. This effect is measurable using proven techniques; so far, with just one SN Ia (SN 1999Q; Figure 10), our results favor the no-dust hypothesis

to better than 2σ [76], but more work along these lines is certainly warranted.

Suppose, though, that for some reason the dust is *very* gray, or our color measurements are not sufficiently precise to rule out Aguirre's (or other) dust. If the cumulative amount of gray dust along the line of sight grows linearly with increasing redshift, we expect that the deviation of the SN Ia peak apparent magnitude from the low- Ω_M , zero- Λ model (Figure 3) will continue growing, to first order (Figure 11). If, on the other hand, the observed faintness of high- z SNe Ia is a consequence of positive Λ , the deviation should actually begin to *decrease* at $z \approx 0.8$ (Figure 11). In essence, we are looking so far back in time that the Λ effect becomes small compared with Ω_M ; the Universe is decelerating at that epoch. Thus, we are embarking on a campaign to find and monitor $z = 0.8\text{--}1.2$ SNe Ia. Given the expected uncertainties (Figure 11), a sample of 10–20 SNe Ia should give a good statistical result.

Note that this test also applies to other systematic effects that grow monotonically with redshift, as may be expected of possible evolution of the white dwarf progenitors (e.g., [66,67]), or gravitational lensing [89]. Indeed, this is our most decisive test to distinguish between Λ and systematic effects. Unless evolution of dust, or of the progenitors, or of the lenses is fixed in such a way as to mimic the effects of Λ (e.g., [71]), our claim of $\Omega_\Lambda > 0$ will become much more convincing if the deviation of apparent magnitude decreases in the expected manner. Such a turnover (Figure 11) can be considered the “smoking gun” of Λ .

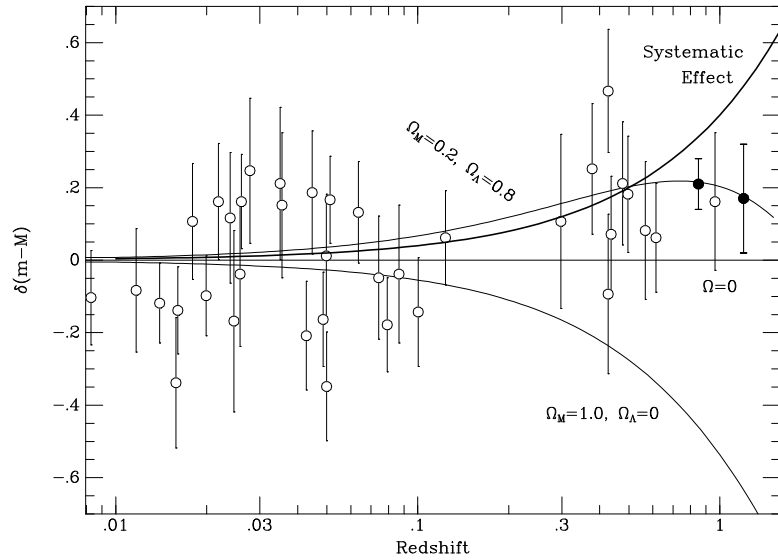


Figure 11: The HZT SN Ia data from Figure 3 (*open circles*) are plotted relative to an empty universe (*horizontal line*). The two faint curves are the best-fitting Λ model, and the $\Omega_M = 1$ ($\Omega_\Lambda = 0$) model. The darker curve shows a systematic bias that increases linearly with z and is consistent with our $z = 0.5$ data. The expected observational uncertainties of hypothetical SNe Ia at redshifts of 0.85 and 1.2 are shown (*filled circles*).

CONCLUSIONS

The luminosity distances of the high-redshift Type Ia supernovae studied by the High-z Supernova Search Team exceed the prediction of a low mass-density ($\Omega_M \approx 0.2$) universe by about 0.25 mag. A cosmological explanation is provided by a positive cosmological constant at roughly the 3σ confidence level, with the prior belief that $\Omega_M \geq 0$. We also find that the expansion of the Universe is currently accelerating ($q_0 \leq 0$, where $q_0 \equiv \Omega_M/2 - \Omega_\Lambda$). The independent results of the Supernova Cosmology Project are fully consistent with these conclusions. Moreover, recent precise measurements of the cosmic microwave background radiation strongly suggest that the Universe is flat ($\Omega_{\text{total}} = \Omega_M + \Omega_\Lambda = 1$); hence, if $\Omega_M \approx 0.3$ (as suggested by many studies, such as of clusters of galaxies), then about 70% of the energy density of the Universe must consist of vacuum energy whose precise nature and evolution are unknown (but definitely not radiation, normal matter, or dark matter). Using the best current values of the Hubble constant, Ω_M , and Ω_Λ , we find that the dynamical age of the Universe is 14.2 ± 1.7 Gyr, including systematic uncertainties in the Cepheid distance scale used for the host galaxies of three nearby SNe Ia. This value is comparable to the derived ages of globular star clusters.

Though the consistent results from the microwave background experiments are reassuring, we are in the process of testing as exhaustively as possible all systematic biases that could be affecting the SN Ia results. For example, qualitative comparisons of spectra of low- z and high- z SNe Ia do not reveal obvious differences, and quantitative tests are in progress. Moreover, the restframe I -band light curves of low- z SNe Ia and a single measured high- z SN Ia look similar, as do their broadband colors. The risetimes of low- z and high- z SNe Ia may differ a little, but the statistical significance of this result is not high, and in any case the early part of the light curve may have little bearing on the peak luminosity. Further tests are in progress. Compelling evidence for acceleration may come in the next few years from a comparison of the peak apparent brightness of $z \gtrsim 0.8$ SNe Ia with the predictions of various models; the signature of nonzero Λ is quite distinct from that of dust, SN evolution, or other effects that grow with redshift.

ACKNOWLEDGMENTS

We thank all of our collaborators in the HZT for their contributions to this work. A.V.F.'s supernova research at U.C. Berkeley is supported by NSF grants AST-9417213 and AST-9987438, and by grants GO-7505 and GO-8177 from the Space Telescope Science Institute, which is operated by the Association of Universities for Research in Astronomy, Inc., under NASA contract NAS 5-26555. A.V.F. is grateful to the meeting organizers for travel funds.

REFERENCES

1. Filippenko, A. V., *ARAA*, **35**, 309 (1997b).
2. Branch, D., & Tammann, G. A., *ARAA*, **30**, 359 (1992).
3. Branch, D., *ARAA*, **36**, 17 (1998).
4. Branch, D., & Miller, D. L., *ApJ*, **405**, L5 (1993).
5. Riess, A. G., *et al.*, *AJ*, **114**, 722 (1997).
6. Branch, D., Fisher, A., & Nugent, P., *AJ*, **106**, 2383 (1993).
7. Vaughan, T. E., Branch, D., Miller, D. L., & Perlmutter, S., *ApJ*, **439**, 558 (1995).
8. Sandage, A., *et al.*, *ApJ*, **460**, L15 (1996).
9. Saha, A., *et al.*, *ApJ*, **486**, 1 (1997).
10. Filippenko, A. V., in *Thermonuclear Supernovae*, ed. P. Ruiz-Lapuente, *et al.* (Dordrecht: Kluwer), p. 1 (1997a).
11. van den Bergh, S., & Pazder, J., *ApJ*, **390**, 34 (1992).
12. Sandage, A., & Tammann, G. A., *ApJ*, **415**, 1 (1993).
13. Filippenko, A. V., *et al.*, *ApJ*, **384**, L15 (1992b).
14. Phillips, M. M., *et al.*, *AJ*, **103**, 1632 (1992).
15. Filippenko, A. V., *et al.*, *AJ*, **104**, 1543 (1992a).
16. Leibundgut, B., *et al.*, *AJ*, **105**, 301 (1993).
17. Turatto, M., *et al.*, *MNRAS*, **283**, 1 (1996).
18. Suntzeff, N., in *Supernovae and Supernova Remnants*, ed. R. McCray & Z. Wang (Cambridge: Cambridge Univ. Press), p. 41 (1996).
19. Li, W. D., *et al.*, in *Cosmic Explosions*, ed. S. S. Holt & W. W. Zhang (New York: American Inst. Physics), p. 91 (2000a).
20. Pskovskii, Yu. P., *Sov. Astron.*, **21**, 675 (1977).
21. Pskovskii, Yu. P., *Sov. Astron.*, **28**, 658 (1984).
22. Branch, D., *ApJ*, **248**, 1076 (1981).
23. Phillips, M. M., *ApJ*, **413**, L105 (1993).
24. Hamuy, M., *et al.*, *AJ*, **109**, 1 (1995).
25. Hamuy, M., *et al.*, *AJ*, **112**, 2398 (1996b).
26. Tripp, R., *A&A*, **325**, 871 (1997).
27. Riess, A. G., Press, W. H., & Kirshner, R. P., *ApJ*, **438**, L17 (1995).
28. Riess, A. G., Press, W. H., & Kirshner, R. P., *ApJ*, **473**, 88 (1996a).
29. Tripp, R., *A&A*, **331**, 815 (1998).
30. Riess, A. G., *et al.*, in preparation (2000b).
31. Hamuy, M., *et al.*, *AJ*, **112**, 2391 (1996a).
32. Branch, D., Romanishin, W., & Baron, E., *ApJ*, **465**, 73; erratum **467**, 473 (1996).
33. Li, W. D., *et al.*, in *Cosmic Explosions*, ed. S. S. Holt & W. W. Zhang (New York: American Inst. Physics), p. 103 (2000b).
34. Filippenko, A. V., *et al.*, in preparation (2000a).
35. Goobar, A., & Perlmutter, S., *ApJ*, **450**, 14 (1995).
36. Norgaard-Nielsen, H., *et al.*, *Nature*, **339**, 523 (1989).
37. Perlmutter, S., *et al.*, *ApJ*, **483**, 565 (1997).
38. Schmidt, B. P., *et al.*, *ApJ*, **507**, 46 (1998).
39. Perlmutter, S., *et al.*, *IAUC* 6270 (1995).

40. Suntzeff, N., *et al.*, *IAUC* 6490 (1996b).
41. Kim, A., Goobar, A., & Perlmutter, S., *PASP*, **108**, 190 (1996).
42. Leibundgut, B., *et al.*, *ApJ*, **466**, L21 (1996).
43. Goldhaber, G., *et al.*, in *Thermonuclear Supernovae*, ed. P. Ruiz-Lapuente, *et al.* (Dordrecht: Kluwer), p. 777 (1997).
44. Filippenko, A. V., *et al.*, in preparation (2000b).
45. Garnavich, P., *et al.*, *ApJ*, **493**, L53 (1998a).
46. Riess, A. G., Nugent, P. E., Filippenko, A. V., Kirshner, R. P., & Perlmutter, S., *ApJ*, **504**, 935 (1998a).
47. Filippenko, A. V., & Riess, A. G., *Physics Reports*, **307**, 31 (1998).
48. Riess, A. G., *et al.*, *AJ*, **116**, 1009 (1998b).
49. Perlmutter, S., *et al.*, *ApJ*, **517**, 565 (1999).
50. Zaldarriaga, M., Spergel, D. N., & Seljak, U. *ApJ*, **488**, 1 (1997).
51. Eisenstein, D. J., Hu, W., & Tegmark, M. *ApJ*, **504**, L57 (1998).
52. Hancock, S., Rocha, G., Lazenby, A. N., & Gutiérrez, C. M., *MNRAS*, **294**, L1 (1998).
53. Lineweaver, C. H., & Barbosa, D., *ApJ*, **496**, 624 (1998).
54. Garnavich, P., *et al.*, *ApJ*, **509**, 74 (1998b).
55. Lineweaver, C. H., *ApJ*, **505**, L69 (1998).
56. Efstathiou, G., *et al.*, *MNRAS*, **303**, L47 (1999).
57. de Bernardis, P., *et al.*, *Nature*, **404**, 955 (2000).
58. Hanany, S., *et al.*, *ApJ*, submitted, astro-ph/0005123 (2000).
59. Balbi, A., *et al.*, *ApJ*, submitted, astro-ph/0005124 (2000).
60. Miller, A. D., *et al.*, *ApJ*, **524**, 1 (1999).
61. Bahcall, N. A., Ostriker, J. P., Perlmutter, S., & Steinhardt, P. J., *Science*, **284**, 1481 (1999).
62. Oswalt, T. D., Smith, J. A., Wood, M. A., & Hintzen, P., *Nature*, **382**, 692 (1996).
63. Cowan, J. J., McWilliam, A., Sneden, C., & Burris, D. L., *ApJ*, **480**, 246 (1997).
64. Gratton, R. G., Fusi Pecci, F., Carretta, E., Clementini, G., Corsi, C. E., & Lattanzi, M., *ApJ*, **491**, 749 (1997).
65. Chaboyer, B., Demarque, P., Kernan, P. J., & Krauss, L. M., *ApJ*, **494**, 96 (1998).
66. Höflich, P., Wheeler, J. C., & Thielemann, F. K., *ApJ*, **495**, 617 (1998).
67. Umeda, H., *et al.*, *ApJ*, **522**, L43 (1999).
68. Domínguez, I., Höflich, P., Straniero, O., & Wheeler, J., in *Future Directions of Supernovae Research: Progenitors to Remnants* (Assergi, Italy), astro-ph/9905047 (1999).
69. Yungelson, L. R., & Livio, M., *ApJ*, **528**, 108 (2000).
70. Nomoto, K., Umeda, H., Hachisu, I., Kato, M., Kobayashi, C., & Tsujimoto, T., in *Type Ia Supernovae: Theory and Cosmology*, ed. J. Truran & J. Niemeyer (Cambridge: Cambridge Univ. Press), in press, astro-ph/9907386 (2000).
71. Drell, P. S., Loredo, T. J., & Wasserman, I., *ApJ*, **530**, 593 (2000).
72. Cappellaro, E., *et al.*, *A&A*, **322**, 431 (1997).
73. Nugent, P., Phillips, M., Baron, E., Branch, D., & Hauschildt, P., *ApJ*, **455**, L147 (1995).
74. Coil, A. L., *et al.*, submitted (2000).

75. Ford, C. H., *et al.*, *AJ*, **106**, 1101 (1993).
76. Riess, A. G., *et al.*, *ApJ*, **536**, 62 (2000).
77. Riess, A. G., *et al.*, *AJ*, **118**, 2675 (1999b).
78. Riess, A. G., Filippenko, A. V., Li, W. D., & Schmidt, B. P., *AJ*, **118**, 2668 (1999a).
79. Goldhaber, G., *et al.*, *BAAS*, **30**, 1325 (1998a).
80. Goldhaber, G., *et al.*, in *Gravity: From the Hubble Length to the Planck Length*, SLAC Summer Institute (Stanford, CA: SLAC) (1998b).
81. Groom, D. E., *BAAS*, **30**, 1419 (1998).
82. Aldering, G., Knop, R., & Nugent, P. *AJ*, **119**, 2110 (2000).
83. Riess, A. G., Press, W. H., & Kirshner, R. P., *ApJ*, **473**, 588 (1996b).
84. Aguirre, A. N., *ApJ*, **512**, L19 (1999a).
85. Hatano, K., Branch, D., & Deaton, J., *ApJ*, **502**, 177 (1998).
86. Bahcall, J. N., *et al.*, *ApJ*, **457**, 19 (1996).
87. Aguirre, A. N., *ApJ*, **525**, 583 (1999b).
88. Aguirre, A., & Haiman, Z., *ApJ*, **525**, 583 (1999).
89. Wambsganss, J., Cen, R., & Ostriker, J. P., *ApJ*, **494**, 29 (1998).